Vibration squeezing and its detection in a single molecular junction

Lei-Lei Nian,[1] Long Bai,[2,*] and Shiqian Hu[1,†]
[1]*School of Physics and Astronomy, Yunnan University, 650091 Kunming, People's Republic of China*
[2]*School of Materials Science and Physics, China University of Mining and Technology, 221116 Xuzhou, People's Republic of China*

(Received 22 February 2023; revised 12 June 2023; accepted 14 June 2023; published 29 June 2023)

How to characterize the electron-vibration interactions at the single-molecule level is a fundamental challenge of molecular electronics. Electron tunneling spectroscopy has so far emerged as one of the powerful tools for witnessing the vibration-mediated electron transport process, while the fluctuation properties of nonthermal vibrations cannot be revealed by simple transport signatures. Here, we study the fluctuation properties of nonthermal vibrations in a current-carrying single molecular junction with or without an external laser radiation. Without the laser drive, the fluctuations of the nonthermal vibrations with sub- and super-Poissonian statistics remain above the zero-point level. When the laser field is turned on, the nonthermal vibrations can be squeezed due to the presence of molecular coherence, where the fluctuations are shown to be reduced below the zero-point level. It is demonstrated that the squeezing and the sub- or super-Poissonian vibration statistics do not always go together. We also propose a cavity engineering to detect the predicted vibration squeezing, where the vibrations and cavity photons are entangled indicated by the two-mode squeezing. This enables optical access to vibration fluctuations in single molecular junctions.

DOI: 10.1103/PhysRevB.107.245428

I. INTRODUCTION

Interest in molecular electronics has rapidly increased since the concept of molecular diodes was proposed by Aviram and Ratner [1]. A single molecule can be connected to two macroscopic electrodes by various techniques, including scanning tunneling microscopy [2,3], mechanically controlled break junctions [4,5], electromigrated molecular junctions [6,7], etc. When a voltage bias is applied between the electrodes, the study of nonequilibrium quantum transport becomes possible in single molecular junctions [8–16]. Some fundamental physics, such as the Coulomb blockade [17], Kondo effect [18], and quantum interference [19–21], can be captured in single-molecule quantum transport. From an application point of view, some electronic devices at the single-molecule level have been proposed, such as transistors [22], switches [23], and diodes [24]. These experiments or proposals have so far mainly concentrated on the transport properties of electrons. Normally, the tunneling electrons are coupled to vibrations in single molecular junctions [25–28]. Signatures of vibration-mediated electron transport can be observed in elastic and inelastic electron tunneling spectroscopy [5,29–31], while the nonequilibrium statistics of vibration degrees of freedom cannot be captured by simple transport measurements.

The statistical properties of vibrations can be characterized theoretically by the Fano factor [32], second-order correlation function [33], and occupation probability [34,35]. A variety of nonthermal vibration states in single molecular junctions [32,33], such as antibunching, bunching, and superbunching, have been demonstrated. However, so far, the fluctuation properties of such nonthermal vibrations are somewhat less well known.

In this paper, we raise a question: Can we reduce the quantum fluctuations of single-molecule nonthermal vibrations below the zero-point quantum noise level of vacuum or coherent state? To address this question, we start from a current-carrying molecular junction with Su-Schrieffer-Heeger-like electron-vibration coupling, and find that the fluctuations of the nonthermal vibrations obeying sub- and super-Poissonian statistics are always above the zero-point level. When an external laser field is applied to the molecule, the nonthermal vibrations can be squeezed where the fluctuations are below the zero-point level, arising from the presence of molecular coherence. The squeezing, which does not always go together with the sub- or super-Poissonian vibration statistics, is demonstrated directly. We further propose a cavity engineering to detect the vibration squeezing, where the vibrations and photons are entangled, and thus one may measure the vibration fluctuations via cavity photons with homodyne techniques.

Our results may possess broad potential applications. First, quantum coherence can be used to engineer nonthermal vibrations into squeezed states without the vibration nonlinearity. Second, the squeezed vibration states are genuinely quantum mechanical in nature, and thus quantum engineering of states at the single molecular level is possible. Third, the reduced variance of displacement or momentum of the nonthermal vibrations allows the realization of ultrasensitive sensors and detectors.

*bailong2200@163.com
†shiqian@ynu.edu.cn

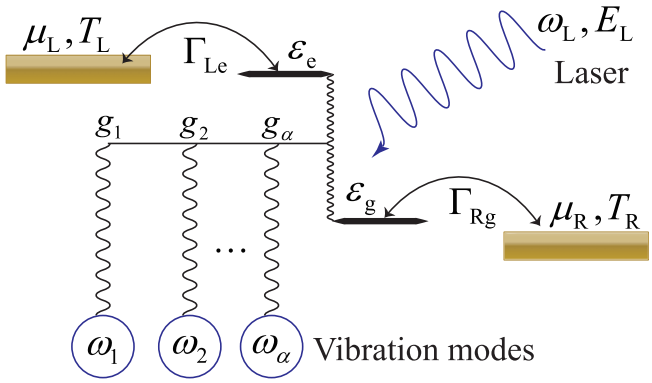

FIG. 1. Schematic drawing of a single molecule with two electrical levels ε_e and ε_g coupled to two electrodes with chemical potential $\mu_{L,R}$ and temperature $T_{L,R}$. The hopping integral between the left electrode and level e is Γ_{Le}, while it is Γ_{Rg} between level g and the right electrode. The electron-vibration coupling, characterized by the strength g_α, leads to vibrational excitation with frequency ω_α. The electron transport through the junction is mediated by an external laser with frequency ω_L and amplitude E_L.

II. MODEL AND METHOD

We consider a single molecular junction subject to an external laser field (Fig. 1), where the electron-vibration coupling is described by the Su-Schrieffer-Heeger-like model [33,36–42]. We consider the strong Coulomb blockade regime, where only one additional electron can tunnel into the molecule, and then the effective Hilbert space of the electronic part is spanned by three states $|0\rangle = |0, 0\rangle$, $|g\rangle = |1, 0\rangle$, and $|e\rangle = |0, 1\rangle$. The system Hamiltonian is ($\hbar = 1$)

$$H_s(t) = H_m(t) + H_{el} + H_b. \tag{1}$$

The first term on the right-hand side of Eq. (1) is the Hamiltonian of the laser-driven molecule

$$H_m(t) = \sum_{i=g,e} \varepsilon_i d_i^\dagger d_i + 2\cos(\omega_L t)(E_L^* d_g^\dagger d_e + E_L d_e^\dagger d_g) + \sum_\alpha \omega_\alpha a_\alpha^\dagger a_\alpha + \sum_\alpha g_\alpha (d_g^\dagger d_e + d_e^\dagger d_g)(a_\alpha^\dagger + a_\alpha), \tag{2}$$

where $d_i^\dagger = |i\rangle\langle 0|$ ($d_i = |0\rangle\langle i|$) creates (destroys) an electron on the level i with energy ε_i. The electron tunneling in the molecule is mediated by an external laser field with frequency ω_L and amplitude E_L. The vibrations are modeled as harmonic oscillators with creation (annihilation) operator $a_\alpha^\dagger$ (a_α) and frequency ω_α, which are linearly coupled to the electronic degrees of freedom with strength g_α. We further consider the laser-electron and electron-vibration couplings in the rotating-wave approximation, and then electron tunneling in the molecule is induced by $E_L^* e^{i\omega_L t} d_g^\dagger d_e + E_L e^{-i\omega_L t} d_e^\dagger d_g$ and $\sum_\alpha g_\alpha (d_g^\dagger d_e a_\alpha^\dagger + d_e^\dagger d_g a_\alpha)$. The second term in Eq. (1) is the Hamiltonian for electrons in electrodes and their coupling with the molecule

$$H_{el} = \sum_{vk} \varepsilon_{vk} c_{vk}^\dagger c_{vk} + \sum_{vk,i} (t_{vk,i} c_{vk}^\dagger d_i + t_{vk,i}^* d_i^\dagger c_{vk}), \tag{3}$$

where $c_{vk}^\dagger$ (c_{vk}) is the creation (annihilation) operator of an electron with wave vector k and energy ε_{vk} in electrode v. The electron tunneling rate between the electrode and molecule is described by $t_{vk,i}$, where $v = L$ for $i = e$ and $v = R$ for $i = g$. The last term in Eq. (1) stands for the bath and its coupling with vibration modes

$$H_b = \sum_{\alpha\beta_\alpha} \omega_{\beta_\alpha} b_{\beta_\alpha}^\dagger b_{\beta_\alpha} + \sum_{\alpha\beta_\alpha} t_{\alpha\beta_\alpha} (a_\alpha^\dagger b_{\beta_\alpha} + a_\alpha b_{\beta_\alpha}^\dagger), \tag{4}$$

where $b_{\beta_\alpha}^\dagger$ (b_{β_α}) is the creation (annihilation) operator of the bath with frequency ω_{β_α}, and $t_{\alpha\beta_\alpha}$ is the vibration-bath coupling strength.

The dynamics of the molecular system follows the Lindblad master equation [43–45]

$$\frac{d}{dt}\rho(t) = -i[H_m(t), \rho(t)] + \mathcal{D}_{el}[\rho(t)] + \mathcal{D}_b[\rho(t)], \tag{5}$$

where $\rho(t)$ is system density matrix and its coherent evolution depends on $H_m(t)$. The dissipative parts of the dynamics, induced by the coupling with the electrode and bath, are described by $\mathcal{D}_{el}[\rho(t)] = \sum_{v,i} \Gamma_{vi}\{f_v(\varepsilon_i)\mathcal{D}[d_i^\dagger, \rho(t)] + \widetilde{f}_v(\varepsilon_i)\mathcal{D}[d_i, \rho(t)]\}$ and $\mathcal{D}_b[\rho(t)] = \sum_\alpha \kappa_\alpha\{n_B(\omega_\alpha)\mathcal{D}[a_\alpha^\dagger, \rho(t)] + \widetilde{n}_B(\omega_\alpha)\mathcal{D}[a_\alpha, \rho(t)]\}$, where $\widetilde{f}_v(\varepsilon_i) = 1 - f_v(\varepsilon_i)$ and $\widetilde{n}_B(\omega_\alpha) = 1 + n_B(\omega_\alpha)$. $\Gamma_{vi}(\varepsilon) = 2\pi \sum_k |t_{vk,i}|^2 \delta(\varepsilon - \varepsilon_{vk})$ and $\kappa_\alpha(\omega) = 2\pi \sum_{\beta_\alpha} |t_{\alpha\beta_\alpha}|^2 \delta(\omega - \omega_{\beta_\alpha})$ are the spectral functions, and we have ignored their energy dependence here. $f_v(\varepsilon_i) = [e^{(\varepsilon_i - \mu_v)/k_B T_v} + 1]^{-1}$ is the Fermi-Dirac distribution of electrode v with chemical potential μ_v and temperature T_v. The mean excitation number of the vibration mode in equilibrium state at temperature T_b is described by the Bose-Einstein distribution $n_B(\omega_\alpha) = [e^{\hbar\omega_\alpha/k_B T_b} - 1]^{-1}$. The Lindblad term is defined as $\mathcal{D}[O, \rho(t)] = [2O\rho(t)O^\dagger - O^\dagger O\rho(t) - \rho(t)O^\dagger O]/2$ with arbitrary operator O.

Since the laser field only contains a single oscillatory component, we can find a rotating frame with the laser frequency ω_L. By introducing a unitary operator $\mathcal{U}(t) = \exp\{-i\omega_L t[\sum_\alpha a_\alpha^\dagger a_\alpha + (d_e^\dagger d_e - d_g^\dagger d_g)/2]\}$, the transformation $\rho^r(t) = \mathcal{U}^\dagger(t)\rho(t)\mathcal{U}(t)$ yields

$$\frac{d}{dt}\rho^r(t) = -i[\mathcal{H}_m, \rho^r(t)] + \mathcal{D}_{el}[\rho^r(t)] + \mathcal{D}_b[\rho^r(t)], \tag{6}$$

where $\mathcal{H}_m = \Delta_m(d_e^\dagger d_e - d_g^\dagger d_g)/2 + \sum_\alpha \Delta_\alpha a_\alpha^\dagger a_\alpha + \sum_\alpha g_\alpha (d_g^\dagger d_e a_\alpha^\dagger + d_e^\dagger d_g a_\alpha) + E_L^* d_g^\dagger d_e + E_L d_e^\dagger d_g$ with frequency detunings $\Delta_m = \omega_m - \omega_L$ ($\omega_m = 2\varepsilon_e = -2\varepsilon_g$) and $\Delta_\alpha = \omega_\alpha - \omega_L$. The dissipative parts of $\mathcal{D}_{el}[\rho^r(t)]$ and $\mathcal{D}_b[\rho^r(t)]$ are unchanged in the rotating frame.

The matrix elements of the molecule density operator $\rho^r(t)$ can be defined as

$$\rho_{\boldsymbol{m},\boldsymbol{n}}^{r,ij}(t) = \langle \boldsymbol{m}, i|\rho^r(t)|j, \boldsymbol{n}\rangle, \tag{7}$$

where $i, j = 0, g, e$ are the empty, ground, and excited states of the electronic system. $\boldsymbol{m} = \{m_1 \cdots m_\alpha\}$ and $\boldsymbol{n} = \{n_1 \cdots n_\alpha\}$ are the vibrational Fock states. Then the matrix elements are

given by

$$\frac{d}{dt}\rho^{r,00}_{\boldsymbol{m},\boldsymbol{n}}(t) = -i\sum_\alpha \Delta_\alpha(m_\alpha - n_\alpha)\rho^{r,00}_{\boldsymbol{m},\boldsymbol{n}}(t) + \mathcal{B}^{00}(t) - [\Gamma_{\rm Le}f_{\rm L}(\varepsilon_{\rm e}) + \Gamma_{\rm Rg}f_{\rm R}(\varepsilon_{\rm g})]\rho^{r,00}_{\boldsymbol{m},\boldsymbol{n}}(t) + \Gamma_{\rm Le}\widetilde{f}_{\rm L}(\varepsilon_{\rm e})\rho^{r,ee}_{\boldsymbol{m},\boldsymbol{n}}(t) + \Gamma_{\rm Rg}\widetilde{f}_{\rm R}(\varepsilon_{\rm g})\rho^{r,gg}_{\boldsymbol{m},\boldsymbol{n}}(t), \quad (8)$$

$$\frac{d}{dt}\rho^{r,gg}_{\boldsymbol{m},\boldsymbol{n}}(t) = -i\sum_\alpha \Delta_\alpha(m_\alpha - n_\alpha)\rho^{r,gg}_{\boldsymbol{m},\boldsymbol{n}} + \mathcal{B}^{gg}(t) + \Gamma_{\rm Rg}\big[f_{\rm R}(\varepsilon_{\rm g})\rho^{r,00}_{\boldsymbol{m},\boldsymbol{n}}(t) - \widetilde{f}_{\rm R}(\varepsilon_{\rm g})\rho^{r,gg}_{\boldsymbol{m},\boldsymbol{n}}(t)\big] - i\big[E^*_{\rm L}\rho^{r,eg}_{\boldsymbol{m},\boldsymbol{n}}(t) - E_{\rm L}\rho^{r,ge}_{\boldsymbol{m},\boldsymbol{n}}(t)\big] - i\sum_\alpha g_\alpha\big[\sqrt{m_\alpha}\rho^{r,eg}_{\widetilde{\boldsymbol{m}}-1,\boldsymbol{n}}(t) - \sqrt{n_\alpha}\rho^{r,ge}_{\boldsymbol{m},\widetilde{\boldsymbol{n}}-1}(t)\big], \quad (9)$$

$$\frac{d}{dt}\rho^{r,ee}_{\boldsymbol{m},\boldsymbol{n}}(t) = -i\sum_\alpha \Delta_\alpha(m_\alpha - n_\alpha)\rho^{r,ee}_{\boldsymbol{m},\boldsymbol{n}}(t) + \mathcal{B}^{ee}(t) + \Gamma_{\rm Le}\big[f_{\rm L}(\varepsilon_{\rm e})\rho^{r,00}_{\boldsymbol{m},\boldsymbol{n}}(t) - \widetilde{f}_{\rm L}(\varepsilon_{\rm e})\rho^{r,ee}_{\boldsymbol{m},\boldsymbol{n}}(t)\big] - i\big[E_{\rm L}\rho^{r,ge}_{\boldsymbol{m},\boldsymbol{n}}(t) - E^*_{\rm L}\rho^{r,eg}_{\boldsymbol{m},\boldsymbol{n}}(t)\big] - i\sum_\alpha g_\alpha\big[\sqrt{m_\alpha+1}\rho^{r,ge}_{\widetilde{\boldsymbol{m}}+1,\boldsymbol{n}}(t) - \sqrt{n_\alpha+1}\rho^{r,eg}_{\boldsymbol{m},\widetilde{\boldsymbol{n}}+1}(t)\big], \quad (10)$$

$$\frac{d}{dt}\rho^{r,ge}_{\boldsymbol{m},\boldsymbol{n}}(t) = -i\sum_\alpha \Delta_\alpha(m_\alpha - n_\alpha)\rho^{r,ge}_{\boldsymbol{m},\boldsymbol{n}}(t) + i\Delta_{\rm m}\rho^{r,ge}_{\boldsymbol{m},\boldsymbol{n}}(t) + \mathcal{B}^{ge}(t) - \frac{1}{2}[\Gamma_{\rm Le}\widetilde{f}_{\rm L}(\varepsilon_{\rm e}) + \Gamma_{\rm Rg}\widetilde{f}_{\rm R}(\varepsilon_{\rm g})]\rho^{r,ge}_{\boldsymbol{m},\boldsymbol{n}}(t) - i\big[E^*_{\rm L}\rho^{r,ee}_{\boldsymbol{m},\boldsymbol{n}}(t) - E^*_{\rm L}\rho^{r,gg}_{\boldsymbol{m},\boldsymbol{n}}(t)\big] - i\sum_\alpha g_\alpha\big[\sqrt{m_\alpha}\rho^{r,ee}_{\widetilde{\boldsymbol{m}}-1,\boldsymbol{n}}(t) - \sqrt{n_\alpha+1}\rho^{r,gg}_{\boldsymbol{m},\widetilde{\boldsymbol{n}}+1}(t)\big], \quad (11)$$

$$\frac{d}{dt}\rho^{r,eg}_{\boldsymbol{m},\boldsymbol{n}}(t) = -i\sum_\alpha \Delta_\alpha(m_\alpha - n_\alpha)\rho^{r,eg}_{\boldsymbol{m},\boldsymbol{n}}(t) - i\Delta_{\rm m}\rho^{r,eg}_{\boldsymbol{m},\boldsymbol{n}}(t) + \mathcal{B}^{eg}(t) - \frac{1}{2}[\Gamma_{\rm Le}\widetilde{f}_{\rm L}(\varepsilon_{\rm e}) + \Gamma_{\rm Rg}\widetilde{f}_{\rm R}(\varepsilon_{\rm g})]\rho^{r,eg}_{\boldsymbol{m},\boldsymbol{n}}(t) - i\big[E_{\rm L}\rho^{r,gg}_{\boldsymbol{m},\boldsymbol{n}}(t) - E_{\rm L}\rho^{r,ee}_{\boldsymbol{m},\boldsymbol{n}}(t)\big] - i\sum_\alpha g_\alpha\big[\sqrt{m_\alpha+1}\rho^{r,gg}_{\widetilde{\boldsymbol{m}}+1,\boldsymbol{n}}(t) - \sqrt{n_\alpha}\rho^{r,ee}_{\boldsymbol{m},\widetilde{\boldsymbol{n}}-1}(t)\big], \quad (12)$$

with

$$\mathcal{B}^{ij}(t) = \sum_\alpha \frac{\kappa_\alpha}{2}\big\{n_{\rm B}(\omega_\alpha)\big[2\sqrt{m_\alpha n_\alpha}\rho^{r,ij}_{\widetilde{\boldsymbol{m}}-1,\widetilde{\boldsymbol{n}}-1}(t) - (m_\alpha + n_\alpha + 2)\rho^{r,ij}_{\boldsymbol{m},\boldsymbol{n}}(t)\big] + \widetilde{n}_{\rm B}(\omega_\alpha)\big[2\sqrt{(m_\alpha+1)(n_\alpha+1)}\rho^{r,ij}_{\widetilde{\boldsymbol{m}}+1,\widetilde{\boldsymbol{n}}+1}(t) - (m_\alpha + n_\alpha)\rho^{r,ij}_{\boldsymbol{m},\boldsymbol{n}}(t)\big]\big\}, \quad (13)$$

where $\widetilde{\boldsymbol{m}} \pm 1 := \{m_1 \pm 1 \cdots m_\alpha\}$ for mode 1 and $\widetilde{\boldsymbol{m}} \pm 1 := \{m_1, m_2 \pm 1 \cdots m_\alpha\}$ for mode 2, similarly for other modes. In the steady state for $t \to \infty$, $\frac{d}{dt}\rho^{r,ij}_{\boldsymbol{m},\boldsymbol{n}}(t) = 0$, we can get time-independent matrix elements $\rho^{r,ij}_{\boldsymbol{m},\boldsymbol{n}}$ with the normalization condition $\mathrm{Tr}[\rho^r] = 1$.

III. VIBRATION SQUEEZING

The dimensionless displacement and momentum operators of the vibration modes are defined as $x_\alpha = (a^\dagger_\alpha + a_\alpha)/\sqrt{2}$ and $p_\alpha = i(a^\dagger_\alpha - a_\alpha)/\sqrt{2}$. They satisfy the commutation rule $[x_\alpha, p_\alpha] = i$, and the corresponding uncertainty relation associated with the relation is given by $\Delta x^2_\alpha \Delta p^2_\alpha \geqslant \frac{1}{4}$, where $\Delta x^2_\alpha = \langle x^2_\alpha\rangle - \langle x_\alpha\rangle^2$ and $\Delta p^2_\alpha = \langle p^2_\alpha\rangle - \langle p_\alpha\rangle^2$ are the variances. The variances can be expressed by the operators $a^\dagger_\alpha$ and a_α,

$$\Delta x^2_\alpha = \tfrac{1}{2}\big[1 + \langle a^{\dagger 2}_\alpha\rangle + \langle a^2_\alpha\rangle + 2\langle a^\dagger_\alpha a_\alpha\rangle - (\langle a^\dagger_\alpha\rangle + \langle a_\alpha\rangle)^2\big], \quad (14)$$

$$\Delta p^2_\alpha = \tfrac{1}{2}\big[1 - \langle a^{\dagger 2}_\alpha\rangle - \langle a^2_\alpha\rangle + 2\langle a^\dagger_\alpha a_\alpha\rangle + (\langle a^\dagger_\alpha\rangle - \langle a_\alpha\rangle)^2\big]. \quad (15)$$

The displacement or momentum is said to be squeezed if $\Delta x^2_\alpha < \frac{1}{2}$ or $\Delta p^2_\alpha < \frac{1}{2}$ [46,47]. When the squeezing occurs, the quantum fluctuations in displacement are reduced below the zero-point quantum noise level of vacuum or coherent state at the expense of increasing fluctuations in momentum, and vice versa.

Before showing the numerical results, we discuss two limiting cases, which can be treated semianalytically, and further provide us a qualitative picture for the origin of vibration squeezing. In the limit $T_v = T_{\rm b} = 0$ and $\mu_{\rm L} \gg \varepsilon_{\rm e} > \varepsilon_{\rm g} \gg \mu_{\rm R}$, we have

$$\frac{d}{dt}\langle a^\dagger_\alpha a_\alpha\rangle = -ig_\alpha(\langle a^\dagger_\alpha d^\dagger_{\rm g} d_{\rm e}\rangle - \langle d^\dagger_{\rm e} d_{\rm g} a_\alpha\rangle) - \kappa_\alpha\langle a^\dagger_\alpha a_\alpha\rangle, \quad (16)$$

$$\frac{d}{dt}\langle a_\alpha\rangle = -i[\Delta_\alpha\langle a_\alpha\rangle + g_\alpha\langle d^\dagger_{\rm g} d_{\rm e}\rangle] - \frac{1}{2}\kappa_\alpha\langle a_\alpha\rangle, \quad (17)$$

$$\frac{d}{dt}\langle a^2_\alpha\rangle = -i\big[2\Delta_\alpha\langle a^2_\alpha\rangle + 2g_\alpha\langle a_\alpha d^\dagger_{\rm g} d_{\rm e}\rangle\big] - \kappa_\alpha\langle a^2_\alpha\rangle, \quad (18)$$

and in the resonance limit $\Delta_\alpha = 0$, the variances in the steady state are therefore given by

$$\Delta x^2_\alpha = \frac{1}{2} + \frac{2g_\alpha(\mathrm{Im}\langle a^\dagger_\alpha d^\dagger_{\rm g} d_{\rm e}\rangle + \mathrm{Im}\langle a_\alpha d^\dagger_{\rm g} d_{\rm e}\rangle)}{\kappa_\alpha} - \frac{8g^2_\alpha(\mathrm{Im}\langle d^\dagger_{\rm g} d_{\rm e}\rangle)^2}{\kappa^2_\alpha}, \quad (19)$$

$$\Delta p^2_\alpha = \frac{1}{2} + \frac{2g_\alpha(\mathrm{Im}\langle a^\dagger_\alpha d^\dagger_{\rm g} d_{\rm e}\rangle - \mathrm{Im}\langle a_\alpha d^\dagger_{\rm g} d_{\rm e}\rangle)}{\kappa_\alpha} - \frac{8g^2_\alpha(\mathrm{Re}\langle d^\dagger_{\rm g} d_{\rm e}\rangle)^2}{\kappa^2_\alpha}. \quad (20)$$

This formula clearly encodes the dependence of Δx^2_α and Δp^2_α on $\langle a^\dagger_\alpha d^\dagger_{\rm g} d_{\rm e}\rangle$, $\langle a_\alpha d^\dagger_{\rm g} d_{\rm e}\rangle$, and $\langle d^\dagger_{\rm g} d_{\rm e}\rangle$. By using Eqs. (8)–(13), we can calculate $\langle a^\dagger_\alpha d^\dagger_{\rm g} d_{\rm e}\rangle = \sum_{\boldsymbol{m}}\sqrt{m_\alpha}\rho^{r,eg}_{\widetilde{\boldsymbol{m}}-1,\boldsymbol{m}}$, $\langle a_\alpha d^\dagger_{\rm g} d_{\rm e}\rangle =$

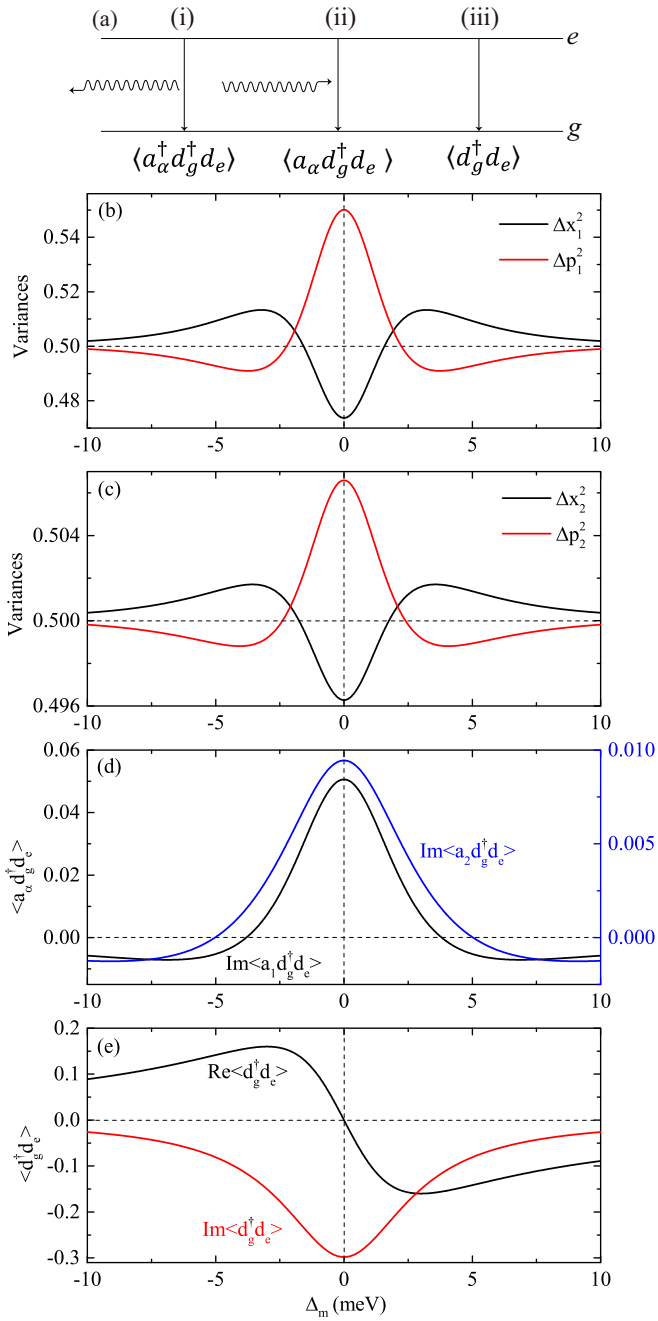

FIG. 2. (a) Transition diagram of electrons for (i) $\langle a_\alpha^\dagger d_g^\dagger d_e\rangle$, (ii) $\langle a_\alpha d_g^\dagger d_e\rangle$, and (iii) $\langle d_g^\dagger d_e\rangle$. (b) and (c) Displacement variance Δx_α^2 and momentum variance Δp_α^2 as a function of the molecule-laser detuning Δ_m. (d) and (e) Similar to (b) and (c), but for $\langle a_\alpha d_g^\dagger d_e\rangle$ and $\langle d_g^\dagger d_e\rangle$ vs Δ_m. Other parameters: $\Delta_1 = \Delta_2 = 0$, $g_1 = 2.5$ meV, $g_2 = 1.5$ meV, $\kappa_1 = 5$ meV, $\kappa_2 = 10$ meV, and $E_L = 1$ meV.

$\sum_{\boldsymbol{m}} \sqrt{m_\alpha + 1}\rho^{r,eg}_{\tilde{\boldsymbol{m}}+1,\boldsymbol{m}}$, and $\langle d_g^\dagger d_e\rangle = \sum_{\boldsymbol{m}} \rho^{r,eg}_{\boldsymbol{m},\boldsymbol{m}}$. As we show in Fig. 2(a), $\langle a_\alpha^\dagger d_g^\dagger d_e\rangle$ corresponds to vibration excitation induced by the inelastic electron tunneling from level e to g. Similar electron tunneling processes also contribute to $\langle a_\alpha d_g^\dagger d_e\rangle$ and $\langle d_g^\dagger d_e\rangle$. For $E_L = 0$, only process (i) is allowed, while processes (ii) and (iii) only occur for $E_L \neq 0$. Thus, in our model, the certain case where the vibration squeezing cannot be generated is $E_L = 0$, which, using Eqs. (19) and (20), gives $\Delta x_\alpha^2 = \Delta p_\alpha^2 = \langle a_\alpha^\dagger a_\alpha\rangle + \frac{1}{2} \geqslant \frac{1}{2}$. This means that the laser-induced correlation ($\langle a_\alpha d_g^\dagger d_e\rangle$) and molecular coherence ($\langle d_g^\dagger d_e\rangle$) play a crucial role in achieving vibration squeezing.

To test our analytical findings, we consider here the case of a molecular junction with two vibration modes. Based on the experimentally and theoretically relevant values [30,48–62], we take $\omega_\alpha = 100$ meV, $\omega_m = 100$ meV, $\Gamma_{Le} = 200$ μeV, $\Gamma_{Rg} = 2$ μeV, $\kappa_\alpha = 5$ meV, and $g_\alpha = 2.5$ meV. A terahertz pulse may be used to mediate the inelastic electron transport in the molecular junctions [63–66]. The asymmetric molecule-electrode coupling can be achieved in scanning tunneling microscope junctions [50,62,67], where the molecule can be decoupled from the metal substrate by introducing an ultrathin insulating Al_2O_3 or NaCl film.

Figures 2(b) and 2(c) show the variances of displacement and momentum (Δx_α^2 and Δp_α^2) as a function of the detuning Δ_m. At a given uncertainty relation, the squeezing of displacement or momentum can be generated depending on Δ_m. For $\Delta_m = 0$, the resonance only results in the squeezing of displacement, where $\mathrm{Im}\langle a_\alpha d_g^\dagger d_e\rangle \neq 0$, $\mathrm{Re}\langle d_g^\dagger d_e\rangle = 0$, and $\mathrm{Im}\langle d_g^\dagger d_e\rangle \neq 0$, as shown in Figs. 2(d) and 2(e). Note that the momentum squeezing of mode 1 can be achieved when $\mathrm{Im}\langle a_1 d_g^\dagger d_e\rangle = 0$ and $\mathrm{Re}\langle d_g^\dagger d_e\rangle \neq 0$, similarly for mode 2. Thus, we highlight that the squeezing is obtained only when the molecular coherence exists. The underlying mechanism is as follows. The laser field allows the electron tunneling from level e to g without emitting a vibration, and thus the molecular coherence is built with the appearance of $\rho^{r,eg}_{\boldsymbol{m},\boldsymbol{m}}$ in Eq. (12). Such a tunneling event also results in the emission of vibrations, which is accompanied by the generations of $\rho^{r,ii}_{\tilde{\boldsymbol{m}}+1,\boldsymbol{m}}$ and $\rho^{r,ii}_{\tilde{\boldsymbol{m}}+2,\boldsymbol{m}}$. Consequently, contributions from $\langle a_\alpha\rangle$ and $\langle a_\alpha^2\rangle$ to Δx_α^2 and Δp_α^2 are then added, giving rise to the squeezing of displacement or momentum. Similar mechanisms for the laser-driven plasmon squeezing have been observed in single molecular junctions [68]. It is worth mentioning that our discussion is different from that of Refs. [69,70], where the vibration squeezing is driven by the Josephson current and tunneling current, respectively.

We further study the robustness of the squeezing under molecule-electrode induced decoherence. For $E_L = 0$, an electron injected from the left electrode occupies the level e, and it can relax to the level g by emitting a vibration and then tunnel to the right electrode. No squeezing is observed due to the absence of molecular coherence. For $E_L \neq 0$, depending on the coupling strength Γ_{Rg}, an electron in the level g can tunnel to the right electrode directly or back to the level e by absorbing a photon. For small Γ_{Rg}, the laser-dominated inelastic electron transitions between levels e and g can take place, resulting in the appearance of significant molecular coherence and thus the squeezing. However, for large Γ_{Rg}, the electron in the level g tends to tunnel to the right electrode. Thus, the laser-mediated transport process becomes suppressed, and the squeezing vanishes because the molecular coherence is broken. The variances Δx_1^2 (Δp_1^2) and Δx_2^2 (Δp_2^2) as a function of Γ_{Rg} are plotted in Figs. 3(a) and 3(b) for different κ_α and g_α. Obviously, the squeezing only survives for small Γ_{Rg}. As the inelastic tunneling of electrons can simultaneously

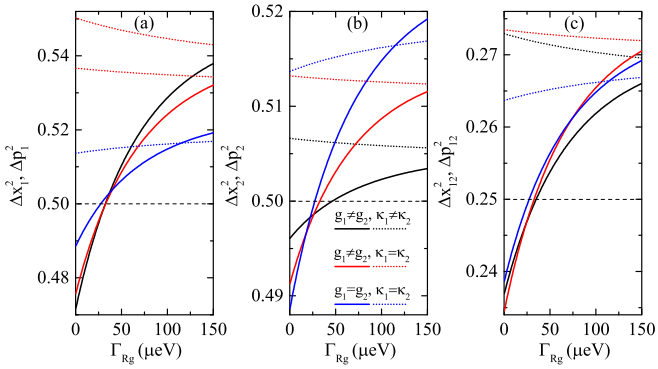

FIG. 3. Variances Δx_α^2, Δp_α^2, Δx_{12}^2, and Δp_{12}^2 as a function of the molecule-electrode coupling Γ_{Rg} for $\Delta_\alpha = \Delta_m = 0$. The solid and dotted lines are for $\Delta x_{\alpha,12}^2$ and $\Delta p_{\alpha,12}^2$, respectively. The other parameters for the black lines are the same as in Fig. 2(b). The red lines correspond to $g_1 = 2.5$ meV, $g_2 = 1.5$ meV, and $\kappa_1 = \kappa_2 = 5$ meV. The blue lines are similar to the red ones but for $g_1 = g_2 = 2.5$ meV.

excite the two vibration modes, the nonlocal correlation can be built. Deeper insight into the correlation can be revealed from the two-mode squeezing, which indicates that the two bosonic modes are entangled [71]. The two-mode quadrature operators are defined as $x_{12} = (a_1^\dagger + a_1 + a_2^\dagger + a_2)/2\sqrt{2}$ and $p_{12} = i(a_1^\dagger - a_1 + a_2^\dagger - a_2)/2\sqrt{2}$. As can be seen in Fig. 3(c), the two-mode vibration squeezing with $\Delta x_{12}^2 < \frac{1}{4}$ can be achieved. A similar line shape and Γ_{Rg} dependence is observed in the contribution of the decoherence to the two-mode squeezing. We note that such a behavior also holds for the off-resonance case with $\Delta_1 \neq \Delta_2 \neq \Delta_m$, as shown in Fig. 4.

Besides the molecule-electrode coupling, the molecular coherence and thus the squeezing are obviously affected by the laser strength E_L. The Δ_0 dependence of the variances are presented in Fig. 5 for different E_L. For small E_L, the bias-driven electron tunneling dominates the transport process, where a significant molecular coherence cannot be established. Then the squeezing is not observed. With increasing the coupling to the laser field, the laser-mediated electron transport becomes enhanced and, consequently, the coherence-induced squeezing can be achieved. Note that, in the high laser-strength regime, the vibration fluctuations will increase above the zero-point level, and the squeezing vanishes.

The vibration-vibration interactions are always present in real molecular junctions. To elucidate the role of vibration-vibration coupling in the squeezing, we introduce the Hamiltonian $H_{v\text{-}v} = J(a_1^\dagger a_2 + a_2^\dagger a_1)$, where J is the coupling strength. Normally, mode coupling can shift the eigenfrequencies of the vibration system. By adding $H_{v\text{-}v}$ into Eq. (1), we find that its effect on the squeezing is to shift the squeezing's position by putting the eigenfrequencies off resonance from the drive (Fig. 6). The magnitude of the squeezing does not significantly change, so in the following we will take $J = 0$.

IV. MULTILEVEL MOLECULAR JUNCTIONS

Above, we limited our discussion to the two-level molecular junctions, while coherence-induced vibration squeezing can be achieved in multilevel cases when the laser-mediated inelastic electron transport process occurs. Taking the

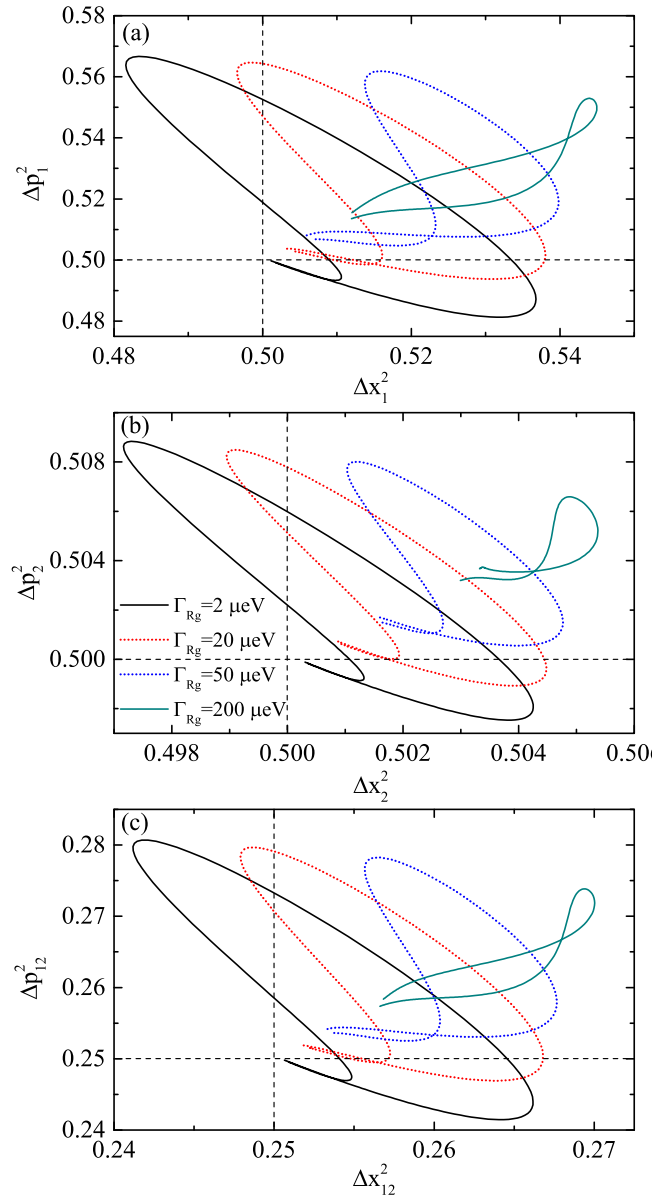

FIG. 4. (a) Phase portrait of Δp_1^2-Δx_1^2 by changing Δ_m with $\Delta_1 = -1.5$ meV and $\Delta_2 = -2$ meV, for indicated values of the molecule-electrode couplings Γ_{Rg}. (b) and (c) Similar to (a), but for Δp_2^2-Δx_2^2 and Δp_{12}^2-Δx_{12}^2. The other parameters are the same as in Fig. 2(b).

three-level case as an example [Fig. 7(a)], the molecular Hamiltonian in the rotating-wave approximation is given by

$$H_m^3(t) = \sum_{i=g,s,e} \varepsilon_i d_i^\dagger d_i + E_L^* e^{i\omega_L t} d_g^\dagger d_s + E_L e^{-i\omega_L t} d_s^\dagger d_g + g_1(d_s^\dagger d_e a_1^\dagger + d_e^\dagger d_s a_1) + g_2(d_g^\dagger d_s a_2^\dagger + d_s^\dagger d_g a_2), \quad (21)$$

where the other parts are the same as the two-level case. The levels g and e are coupled to level s by two vibration modes. The molecular transition from g to s is also mediated by a laser field. For simplicity, we take $\varepsilon_s = 0$ and $\varepsilon_g = -\varepsilon_e$. In

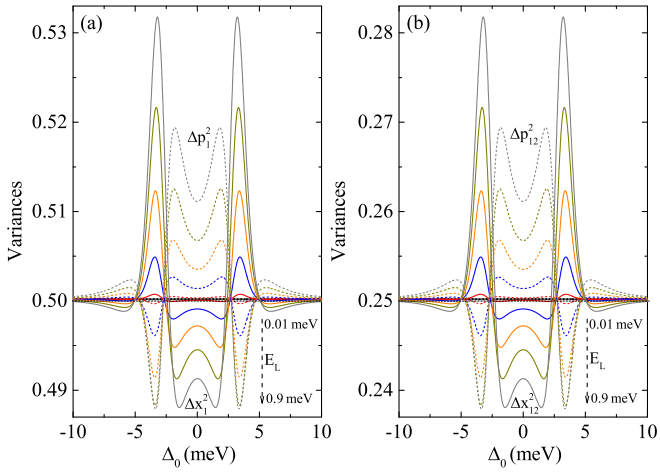

FIG. 5. (a) Variances Δx_1^2 and Δp_1^2 as a function of the detuning $\Delta_0 = \Delta_{\alpha,\mathrm{m}}$ for indicated values of E_L, where $\Delta x_1^2 = \Delta x_2^2$ and $\Delta p_1^2 = \Delta p_2^2$. (b) Similar to (a), but for Δx_{12}^2 and Δp_{12}^2 vs Δ_0. Along the direction of the arrow, the laser amplitudes are $E_\mathrm{L} = (0.01, 0.1, 0.3, 0.5, 0.7, 0.9)$ meV.

the rotating frame, we have

$$\mathcal{H}_\mathrm{m}^3 = \Delta_\mathrm{e}(d_\mathrm{e}^\dagger d_\mathrm{e} - d_\mathrm{g}^\dagger d_\mathrm{g}) + E_\mathrm{L}^* d_\mathrm{g}^\dagger d_\mathrm{s} + E_\mathrm{L} d_\mathrm{s}^\dagger d_\mathrm{g} + g_1(d_\mathrm{s}^\dagger d_\mathrm{e} a_1^\dagger + d_\mathrm{e}^\dagger d_\mathrm{s} a_1) + g_2(d_\mathrm{g}^\dagger d_\mathrm{s} a_2^\dagger + d_\mathrm{s}^\dagger d_\mathrm{g} a_2), \tag{22}$$

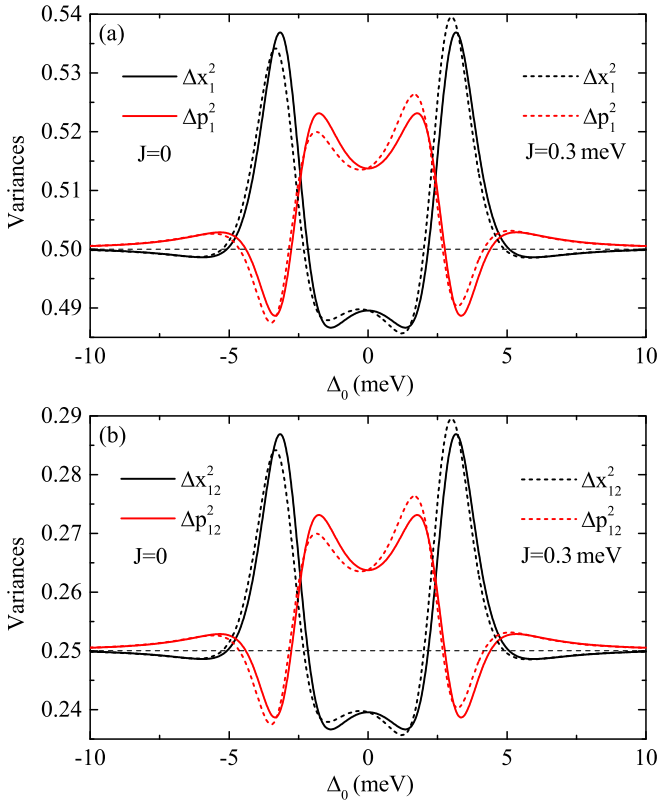

FIG. 6. (a) Variances Δx_1^2 and Δp_1^2 as a function of the detuning $\Delta_0 = \Delta_{\alpha,\mathrm{m}}$ for indicated values of J with $E_\mathrm{L} = 1$ meV, where $\Delta x_1^2 = \Delta x_2^2$ and $\Delta p_1^2 = \Delta p_2^2$. (b) Similar to (a), but for Δx_{12}^2 and Δp_{12}^2 vs Δ_0.

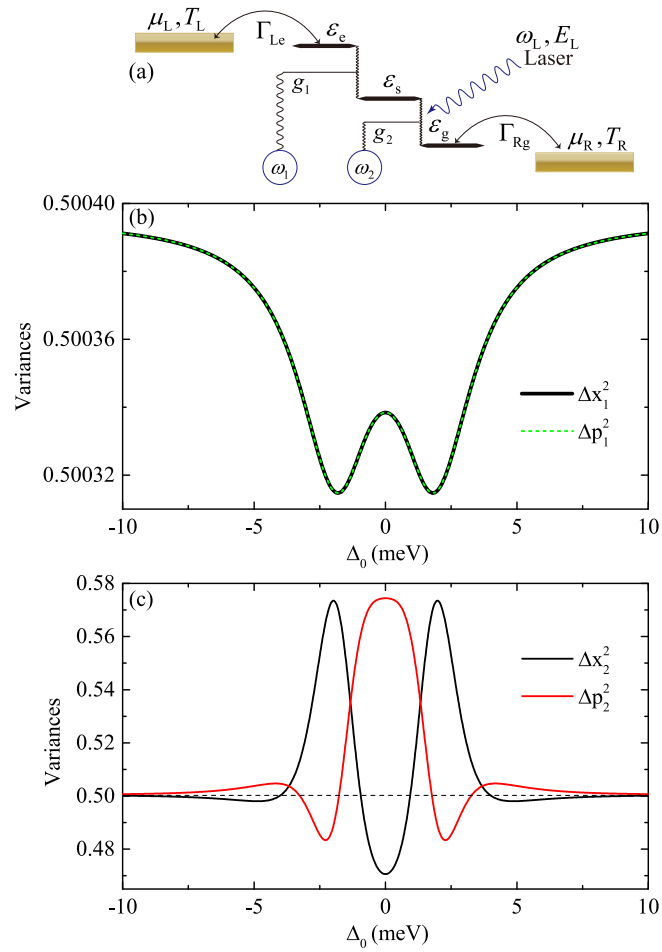

FIG. 7. (a) Schematic of a three-level molecular junction. (b) Variances Δx_1^2 and Δp_1^2 as a function of the detuning $\Delta_0 = \Delta_{\alpha,\mathrm{e}}$ for $E_\mathrm{L} = 1$ meV. (c) Similar to (b), but for Δx_2^2 and Δp_2^2 vs Δ_0.

where $\Delta_\mathrm{e} = \varepsilon_\mathrm{e} - \omega_\mathrm{L}$ is the detuning. By replacing $\mathcal{H}_\mathrm{m}$ with $\mathcal{H}_\mathrm{m}^3$ in Eq. (6), the fluctuation properties of nonthermal vibrations for the three-level case can be obtained from the Δ_0 dependence of variances, which are shown in Fig. 7(b). The electron in the left electrode can tunnel to level e, and it can then relax to level s by emitting a vibration. The laser field is not involved in this transport process, such that the molecular coherence between levels e and s cannot be generated. Therefore, the squeezing of mode 1 is not observed, as indicated by $\Delta x_1^2 > \frac{1}{2}$ and $\Delta p_1^2 > \frac{1}{2}$. The electron in level s can further relax to level g by emitting a vibration. For small Γ_Rg, the electron in level g can absorb a photon and then back to the level s. In such a case, the molecular coherence between levels g and s can be established, which results in the squeezing of mode 2 [Fig. 7(c)]. We see again that the molecular coherence is of key importance as the condition for achieving the squeezing, even in multilevel molecular junctions.

V. VIBRATION SQUEEZING AND STATISTICS

We now discuss the role of vibration statistics in the squeezing. The vibration emission statistics can be characterized by the second-order correlation function

TABLE I. Vibration squeezing and statistics.

	Vibration statistics without laser ($E_L = 0$)			Vibration statistics with laser ($E_L \neq 0$)		
Vibration squeezing	Antibunching	Bunching	Superthermal bunching	Antibunching	Bunching	Superthermal bunching
Mode 1	×	×	×	√	√	√
Mode 2	×	×	×	√	√	√
Mode 1 ↔ 2	×	×	×	√	√	√

$g_\alpha^{(2)}(0) = \langle a_\alpha^\dagger a_\alpha^\dagger a_\alpha a_\alpha\rangle/\langle a_\alpha^\dagger a_\alpha\rangle^2$. To reveal the vibration statistics dependence of the squeezing, we have

$$\Delta x_\alpha^2 = \tfrac{1}{2} + \sqrt{\langle a_\alpha^\dagger a_\alpha^\dagger a_\alpha a_\alpha\rangle/g_\alpha^{(2)}(0)} + \mathrm{Re}\langle a_\alpha^2\rangle - \mathrm{Re}\langle a_\alpha\rangle^2 - \langle a_\alpha^\dagger\rangle\langle a_\alpha\rangle, \tag{23}$$

$$\Delta p_\alpha^2 = \tfrac{1}{2} + \sqrt{\langle a_\alpha^\dagger a_\alpha^\dagger a_\alpha a_\alpha\rangle/g_\alpha^{(2)}(0)} - \mathrm{Re}\langle a_\alpha^2\rangle + \mathrm{Re}\langle a_\alpha\rangle^2 - \langle a_\alpha^\dagger\rangle\langle a_\alpha\rangle, \tag{24}$$

$$\Delta x_{12}^2 = \tfrac{1}{4}\big(\Delta x_1^2 + \Delta x_2^2 + 2\langle x_1 x_2\rangle - 2\langle x_1\rangle\langle x_2\rangle\big), \tag{25}$$

$$\Delta p_{12}^2 = \tfrac{1}{4}\big(\Delta p_1^2 + \Delta p_2^2 + 2\langle p_1 p_2\rangle - 2\langle p_1\rangle\langle p_2\rangle\big). \tag{26}$$

For $E_L = 0$, $\langle a_\alpha\rangle = 0$, $\langle a_\alpha^2\rangle = 0$, and $\langle x_\alpha\rangle = \langle p_\alpha\rangle = 0$, which yields

$$\Delta x_\alpha^2 = \Delta p_\alpha^2 = \tfrac{1}{2} + \sqrt{\langle a_\alpha^\dagger a_\alpha^\dagger a_\alpha a_\alpha\rangle/g_\alpha^{(2)}(0)}, \tag{27}$$

$$\Delta x_{12}^2 = \Delta p_{12}^2 = \tfrac{1}{4}\big(\Delta x_1^2 + \Delta x_2^2 + 2\,\mathrm{Re}\langle a_1^\dagger a_2\rangle\big), \tag{28}$$

where $\langle a_1^\dagger a_2\rangle$ is the current-driven vibration correlation between modes 1 and 2. The results clearly show that the squeezing is impossible without the laser drive, regardless of the vibration statistics. The numerical results in Fig. 8 can further verify this, where for $E_L = 0$ the vibration squeezing vanishes when the current-driven vibrations obey various nonthermal statistics, such as antibunching, bunching, and superthermal bunching. The superthermal vibration bunching is caused by a joint interference effect [72]. For $E_L \neq 0$, the role of vibration statistics in the squeezing cannot be given directly by Eqs. (23)–(26). To show this explicitly, in Fig. 9, the variances and second-order correlation functions are plotted as a function of the detuning Δ_0. Depending on Δ_0, the squeezing of displacement or momentum can be achieved alternately, where the vibrations can obey either sub- or super-Poissonian statistics. Evidently, in the presence of the laser field, the generation of vibration squeezing is statistics independent. As a result, the direct connection between vibration squeezing and statistics can be established, as shown in Table I.

VI. DETECTING VIBRATION SQUEEZING VIA CAVITY ENGINEERING

In principle, it is difficult to directly measure the predicted vibration squeezing in single molecular junctions. The quantum fluctuations of the cavity photons can usually be measured by homodyne techniques [73,74], where the normally ordered variance of the source field can be achieved for characterizing the photon squeezing. Thus, we propose a cavity engineering to detect the vibration squeezing, where the single molecular junction is coupled to a cavity [Fig. 10(a)]. This setup can be realized experimentally in quantum-dot-like circuit quantum electrodynamics [75–78], where the quantum dots play a role similar to the molecule. The Hamiltonian for the coupled molecule-cavity system takes the form

$$\mathcal{H}_{mc} = \Delta_c a_c^\dagger a_c + g_{mc}(d_g^\dagger d_e a_c^\dagger + d_e^\dagger d_g a_c), \tag{29}$$

where $a_c^\dagger$ (a_c) is the creation (annihilation) operator of the cavity photon with angular frequency ω_c. $\Delta_c = \omega_c - \omega_L$ is cavity-laser frequency detuning. In the zero-temperature limit, the cavity-environment coupling is described by $\mathcal{D}_c[\rho^r(t)] = (\kappa_c/2)\mathcal{D}[a_c, \rho^r(t)]$ with the dissipation rate κ_c. g_{mc} is the

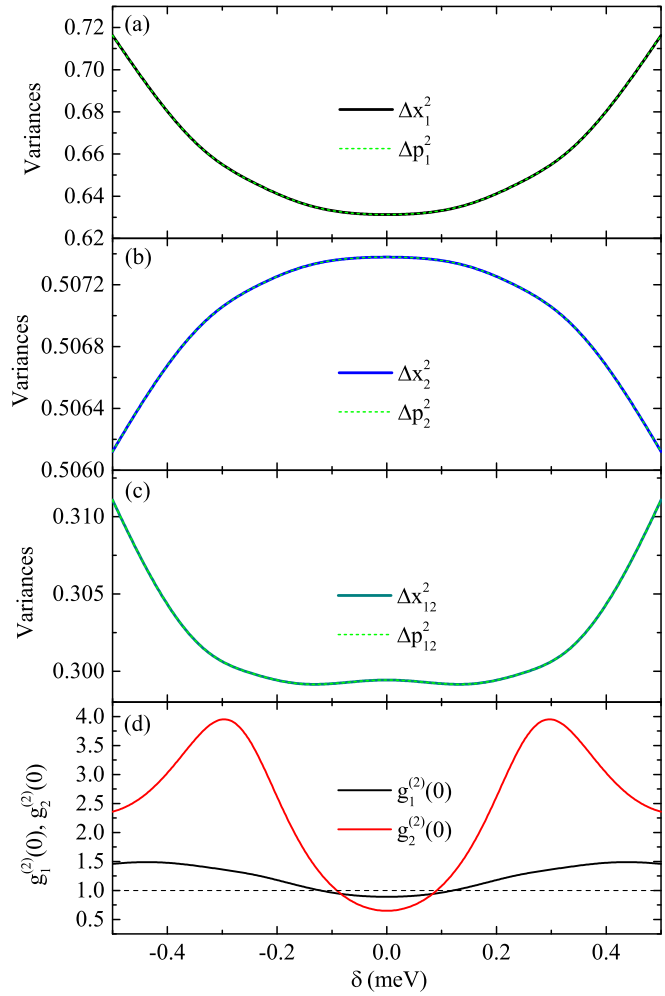

FIG. 8. (a)–(c) Variances Δx_α^2, Δp_α^2, Δx_{12}^2, and Δp_{12}^2 as a function of the detuning δ. (d) Similar to (a)–(c), but for $g_1^{(2)}(0)$ and $g_2^{(2)}(0)$ vs δ. Other parameters: $E_L = 0$, $\omega_2 = \omega_1 + \delta$, $g_1 = 0.4$ meV, $g_2 = 0.1$ meV, $\kappa_1 = 2$ μeV, and $\kappa_2 = 200$ μeV.

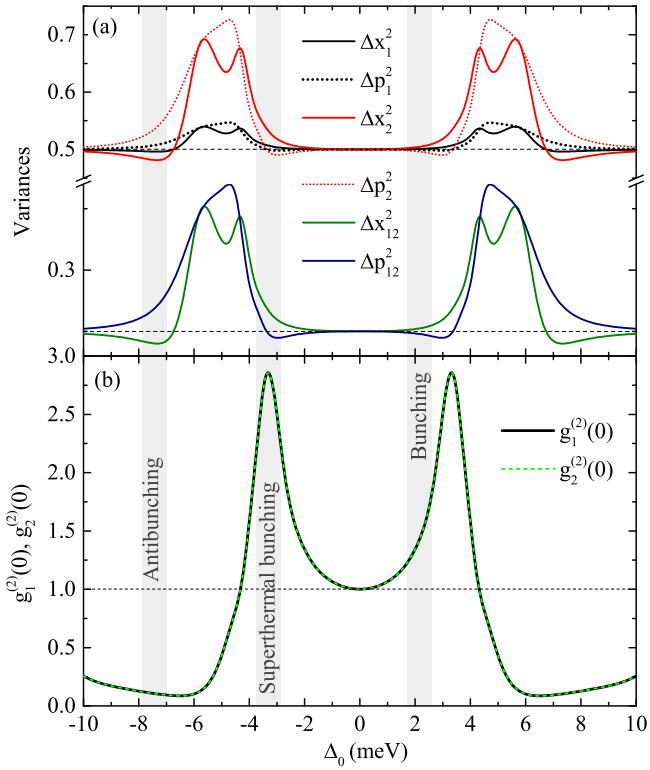

FIG. 9. (a) Variances Δx_α^2, Δp_α^2, Δx_{12}^2, and Δp_{12}^2 as a function of the detuning Δ_0 with $g_2 = 5.5$ meV, $\Gamma_{\rm Rg} = 0.2$ μeV, $\kappa_\alpha = 1$ meV, and $E_{\rm L} = 1$ meV. (b) Similar to (a), but for $g_1^{(2)}(0)$ and $g_2^{(2)}(0)$ vs Δ_0.

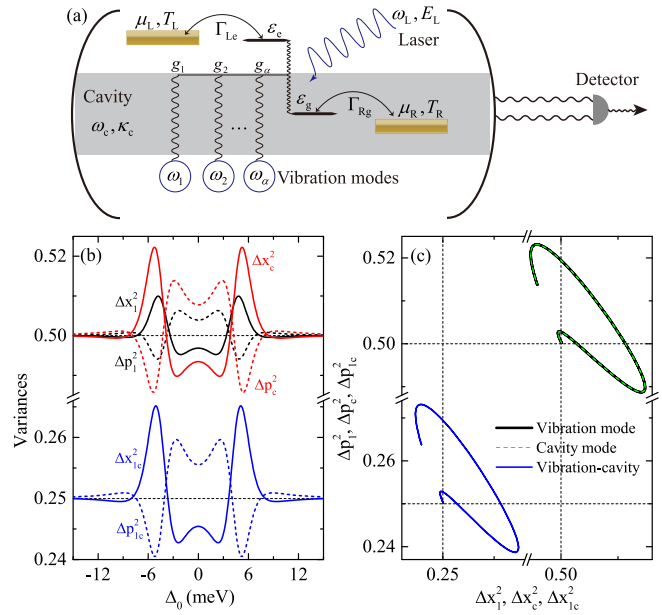

FIG. 10. (a) Schematic illustration of a single molecular junction in a cavity. (b) Variances Δx_1^2, $\Delta x_{\rm c}^2$, Δp_1^2, $\Delta p_{\rm c}^2$, $\Delta x_{1{\rm c}}^2$, and $\Delta p_{1{\rm c}}^2$ as a function of the detuning $\Delta_0 = \Delta_{1,{\rm m},{\rm c}}$ with $\kappa_{\rm c} = 10$ meV, $g_{\rm mc} = 5$ meV, and $E_{\rm L} = 1$ meV. The displacement variance and momentum variance of cavity mode are defined as $\Delta x_{\rm c}^2 = \langle x_{\rm c}^2\rangle - \langle x_{\rm c}\rangle^2$ and $\Delta p_{\rm c}^2 = \langle p_{\rm c}^2\rangle - \langle p_{\rm c}\rangle^2$, where $x_{\rm c} = (a_{\rm c}^\dagger + a_{\rm c})/\sqrt{2}$ and $p_{\rm c} = i(a_{\rm c}^\dagger - a_{\rm c})/\sqrt{2}$. The two-mode squeezing occurs when $\Delta x_{1{\rm c}}^2 < \frac{1}{4}$ or $\Delta p_{1{\rm c}}^2 < \frac{1}{4}$, where $x_{1{\rm c}} = (a_1^\dagger + a_1 + a_{\rm c}^\dagger + a_{\rm c})/2\sqrt{2}$ and $p_{1{\rm c}} = i(a_1^\dagger - a_1 + a_{\rm c}^\dagger - a_{\rm c})/2\sqrt{2}$. (c) Similar to (b), but for phase portraits of $\Delta p_1^2 - \Delta x_1^2$, $\Delta p_{\rm c}^2 - \Delta x_{\rm c}^2$, and $\Delta p_{1{\rm c}}^2 - \Delta c_{1{\rm c}}^2$ with $g_1 = g_{\rm mc}$ and $\kappa_1 = \kappa_{\rm c}$.

molecule-cavity coupling strength. Specifically, taking one-vibration molecular junction as an example, we show in Fig. 10(b) the variances of vibration and cavity modes as a function of detuning Δ_1, calculated by adding Eq. (29) and $\mathcal{D}_{\rm c}[\rho^r(t)]$ into Eq. (6). It is found that the vibration and cavity modes can be squeezed simultaneously. In principle, when the electrons transport inelastically through the molecule, a nonlocal interaction between the vibration and cavity photon will be established as expected, even without the laser field. However, the laser-induced molecular coherence enables the generation of two-mode squeezing, indicating that the vibration and cavity photon are entangled. This provides a feasible way for the detection of vibration fluctuations in single molecular junctions by cavity photons. More importantly, the Δ_1 dependence of the squeezing condition for the vibrations, shown in Fig. 10(c), can follow exactly the dependence of the cavity photons. Thus the precise detection of the vibration fluctuations is consequently achieved.

VII. CONCLUSIONS AND OUTLOOK

The fluctuation properties of nonthermal vibrations is studied in a current-carrying single molecular junction with or without an external laser radiation. We find that the nonthermal vibrations can only be squeezed in a laser-driven molecular junction, where the vibration fluctuations can be reduced below the zero-point level. The squeezing originates from the molecular coherence and does not always go together with sub- or super-Poissonian vibration statistics. When the molecular junction is coupled to a cavity, the entanglement between vibrations and cavity photons allows us to detect the vibration squeezing by photon measurement with homodyne techniques. Our results pave the way to reveal the vibration fluctuations in single molecular junctions.

The molecule-cavity setups have emerged as a promising means to control the molecular properties via the strong light-matter coupling between molecular transition of electronic or vibratonal degrees of freedom and cavity photons, resulting in the generation of polaritonic state [79–83]. To date, the formation of molecular polaritons was utilized in a broad spectrum of applications, ranging from polariton lasing [84] and Bose-Einstein condensation [85] to long-range excitation transport [86] and quantum information technology [87,88]. It is necessary to reveal the role of the molecular polariton in the vibrational fluctuations, with the aim to inspire more explorations to the area of vibration quantum noise modulation. This may promote the intersection of molecular electronics and polaritonics.

ACKNOWLEDGMENTS

This work was funded by the National Natural Science Foundation of China (Grants No. 12204405, No. 12105242, and No. 11104346) and by the Yunnan Fundamental Research Project (Grants No. 202301AT070108, No. 202201AT070161, and No. 202301AW070006).

[1] A. Aviram and M. A. Ratner, Molecular rectifiers, Chem. Phys. Lett. **29**, 277 (1974).

[2] A. Aviram, C. Joachim, and M. Pomerantz, Evidence of switching and rectification by a single molecule effected with a scanning tunneling microscope, Chem. Phys. Lett. **146**, 490 (1988).

[3] B. C. Stipe, M. A. Rezaei, and W. Ho, Single-molecule vibrational spectroscopy and microscopy, Science **280**, 1732 (1998).

[4] M. A. Reed, C. Zhou, C. Muller, T. Burgin, and J. Tour, Conductance of a molecular junction, Science **278**, 252 (1997).

[5] R. Smit, Y. Noat, C. Untiedt, N. Lang, M. v. van Hemert, and J. Van Ruitenbeek, Measurement of the conductance of a hydrogen molecule, Nature (London) **419**, 906 (2002).

[6] L. H. Yu, Z. K. Keane, J. W. Ciszek, L. Cheng, M. P. Stewart, J. M. Tour, and D. Natelson, Inelastic Electron Tunneling via Molecular Vibrations in Single-Molecule Transistors, Phys. Rev. Lett. **93**, 266802 (2004).

[7] S. Sapmaz, P. Jarillo-Herrero, Y. M. Blanter, C. Dekker, and H. S. J. van der Zant, Tunneling in Suspended Carbon Nanotubes Assisted by Longitudinal Phonons, Phys. Rev. Lett. **96**, 026801 (2006).

[8] A. H. Flood, J. F. Stoddart, D. W. Steuerman, and J. R. Heath, Whence molecular electronics? Science **306**, 2055 (2004).

[9] Y. Dubi and M. Di Ventra, Colloquium: Heat flow and thermoelectricity in atomic and molecular junctions, Rev. Mod. Phys. **83**, 131 (2011).

[10] M. Galperin and A. Nitzan, Molecular optoelectronics: The interaction of molecular conduction junctions with light, Phys. Chem. Chem. Phys. **14**, 9421 (2012).

[11] M. Ratner, A brief history of molecular electronics, Nat. Nanotechnol. **8**, 378 (2013).

[12] D. Xiang, X. Wang, C. Jia, T. Lee, and X. Guo, Molecular-scale electronics: From concept to function, Chem. Rev. **116**, 4318 (2016).

[13] M. Thoss and F. Evers, Perspective: Theory of quantum transport in molecular junctions, J. Chem. Phys. **148**, 030901 (2018).

[14] N. Xin, J. Guan, C. Zhou, X. Chen, C. Gu, Y. Li, M. A. Ratner, A. Nitzan, J. F. Stoddart, and X. Guo, Concepts in the design and engineering of single-molecule electronic devices, Nat. Rev. Phys. **1**, 211 (2019).

[15] F. Evers, R. Korytár, S. Tewari, and J. M. van Ruitenbeek, Advances and challenges in single-molecule electron transport, Rev. Mod. Phys. **92**, 035001 (2020).

[16] P. Li, Z. Li, C. Zhao, H. Ju, Q. Gao, W. Si, L. Cheng, J. Hao, M. Li, Y. Chen, C. Jia, and X. Guo, Single-molecule nano-optoelectronics: Insights from physics, Rep. Prog. Phys. **85**, 086401 (2022).

[17] H. Park, J. Park, A. K. Lim, E. H. Anderson, A. P. Alivisatos, and P. L. McEuen, Nanomechanical oscillations in a single-C_{60} transistor, Nature (London) **407**, 57 (2000).

[18] W. Liang, M. P. Shores, M. Bockrath, J. R. Long, and H. Park, Kondo resonance in a single-molecule transistor, Nature (London) **417**, 725 (2002).

[19] H. Vazquez, R. Skouta, S. Schneebeli, M. Kamenetska, R. Breslow, L. Venkataraman, and M. Hybertsen, Probing the conductance superposition law in single-molecule circuits with parallel paths, Nat. Nanotechnol. **7**, 663 (2012).

[20] C. M. Guédon, H. Valkenier, T. Markussen, K. S. Thygesen, J. C. Hummelen, and S. J. Van Der Molen, Observation of quantum interference in molecular charge transport, Nat. Nanotechnol. **7**, 305 (2012).

[21] J. Bai, A. Daaoub, S. Sangtarash, X. Li, Y. Tang, Q. Zou, H. Sadeghi, S. Liu, X. Huang, Z. Tan, J. Liu, Y. Yang, J. Shi, G. Mészáros, W. Chen, C. Lambert, and W. Hong, Anti-resonance features of destructive quantum interference in single-molecule thiophene junctions achieved by electrochemical gating, Nat. Mater. **18**, 364 (2019).

[22] F. Jäckel, M. D. Watson, K. Müllen, and J. P. Rabe, Prototypical Single-Molecule Chemical-Field-Effect Transistor with Nanometer-Sized Gates, Phys. Rev. Lett. **92**, 188303 (2004).

[23] C. Jia, A. Migliore, N. Xin, S. Huang, J. Wang, Q. Yang, S. Wang, H. Chen, D. Wang, B. Feng, Z. Liu, G. Zhang, D.-H. Qu, H. Tian, M. A. Ratner, H. Q. Xu, A. Nitzan, and X. Guo, Covalently bonded single-molecule junctions with stable and reversible photoswitched conductivity, Science **352**, 1443 (2016).

[24] B. Capozzi, J. Xia, O. Adak, E. J. Dell, Z.-F. Liu, J. C. Taylor, J. B. Neaton, L. M. Campos, and L. Venkataraman, Single-molecule diodes with high rectification ratios through environmental control, Nat. Nanotechnol. **10**, 522 (2015).

[25] M. Galperin, M. A. Ratner, and A. Nitzan, Molecular transport junctions: Vibrational effects, J. Phys.: Condens. Matter **19**, 103201 (2007).

[26] J.-T. Lü, H. Zhou, J.-W. Jiang, and J.-S. Wang, Effects of electron-phonon interaction on thermal and electrical transport through molecular nano-conductors, AIP Adv. **5**, 053204 (2015).

[27] D. Segal and B. K. Agarwalla, Vibrational heat transport in molecular junctions, Annu. Rev. Phys. Chem. **67**, 185 (2016).

[28] L.-L. Nian, L. Ma, and J.-T. Lü, Electron transport in single molecular devices, in *Nanogap Electrodes*, edited by T. Li (Wiley, Hoboken, NJ, 2021), Chap. 2, pp. 25–56.

[29] X. H. Qiu, G. V. Nazin, and W. Ho, Vibronic States in Single Molecule Electron Transport, Phys. Rev. Lett. **92**, 206102 (2004).

[30] J. O. Thomas, B. Limburg, J. K. Sowa, K. Willick, J. Baugh, G. A. D. Briggs, E. M. Gauger, H. L. Anderson, and J. A. Mol, Understanding resonant charge transport through weakly coupled single-molecule junctions, Nat. Commun. **10**, 4628 (2019).

[31] G. Czap, Z. Han, P. J. Wagner, and W. Ho, Detection and Characterization of Anharmonic Overtone Vibrations of Single Molecules on a Metal Surface, Phys. Rev. Lett. **122**, 106801 (2019).

[32] X. Zhong and J. C. Cao, Interference effects on vibration-mediated tunneling through interacting degenerate molecular states, J. Phys.: Condens. Matter **21**, 295602 (2009).

[33] T. Wang, L.-L. Nian, and J.-T. Lü, Nonthermal vibrations in biased molecular junctions, Phys. Rev. E **102**, 022127 (2020).

[34] S. Takei, Y. B. Kim, and A. Mitra, Enhanced Fano factor in a molecular transistor coupled to phonons and Luttinger-liquid leads, Phys. Rev. B **72**, 075337 (2005).

[35] R. Härtle and M. Thoss, Vibrational instabilities in resonant electron transport through single-molecule junctions, Phys. Rev. B **83**, 125419 (2011).

[36] J.-T. Lü, P. Hedegård, and M. Brandbyge, Laserlike Vibrational Instability in Rectifying Molecular Conductors, Phys. Rev. Lett. **107**, 046801 (2011).

[37] J.-T. Lü, M. Brandbyge, P. Hedegård, T. N. Todorov, and D. Dundas, Current-induced atomic dynamics, instabilities, and raman signals: Quasiclassical Langevin equation approach, Phys. Rev. B **85**, 245444 (2012).

[38] L. Simine and D. Segal, Vibrational cooling, heating, and instability in molecular conducting junctions: Full counting statistics analysis, Phys. Chem. Chem. Phys. **14**, 13820 (2012).

[39] B. K. Agarwalla, J.-H. Jiang, and D. Segal, Full counting statistics of vibrationally assisted electronic conduction: Transport and fluctuations of thermoelectric efficiency, Phys. Rev. B **92**, 245418 (2015).

[40] B. K. Agarwalla and D. Segal, Reconciling perturbative approaches in phonon-assisted transport junctions, J. Chem. Phys. **144**, 074102 (2016).

[41] G. Foti and H. Vázquez, Origin of vibrational instabilities in molecular wires with separated electronic states, J. Phys. Chem. Lett. **9**, 2791 (2018).

[42] F. Chen, K. Miwa, and M. Galperin, Electronic friction in interacting systems, J. Chem. Phys. **150**, 174101 (2019).

[43] G. Lindblad, On the generators of quantum dynamical semigroups, Commun. Math. Phys. **48**, 119 (1976).

[44] H.-P. Breuer and F. Petruccione, *The Theory of Open Quantum Systems* (Oxford University Press, Oxford, UK, 2002).

[45] H. J. Carmichael, *Statistical Methods in Quantum Optics 1: Master Equations and Fokker-Planck Equations* (Springer, Berlin, 2013).

[46] M. O. Scully and M. S. Zubairy, *Quantum Optics* (Cambridge University Press, Cambridge, UK, 1997).

[47] C. Gerry, P. Knight, and P. L. Knight, *Introductory Quantum Optics* (Cambridge University Press, Cambridge, UK, 2005).

[48] S. W. Wu, G. V. Nazin, X. Chen, X. H. Qiu, and W. Ho, Control of Relative Tunneling Rates in Single Molecule Bipolar Electron Transport, Phys. Rev. Lett. **93**, 236802 (2004).

[49] Z.-C. Dong, X.-L. Guo, A. S. Trifonov, P. S. Dorozhkin, K. Miki, K. Kimura, S. Yokoyama, and S. Mashiko, Vibrationally Resolved Fluorescence from Organic Molecules near Metal Surfaces in a Scanning Tunneling Microscope, Phys. Rev. Lett. **92**, 086801 (2004).

[50] G. Nazin, S. Wu, and W. Ho, Tunneling rates in electron transport through double-barrier molecular junctions in a scanning tunneling microscope, Proc. Natl. Acad. Sci. USA **102**, 8832 (2005).

[51] J. Jiang, M. Kula, W. Lu, and Y. Luo, First-principles simulations of inelastic electron tunneling spectroscopy of molecular electronic devices, Nano Lett. **5**, 1551 (2005).

[52] M. Galperin, A. Nitzan, and M. A. Ratner, Heat conduction in molecular transport junctions, Phys. Rev. B **75**, 155312 (2007).

[53] L. Vitali, R. Ohmann, K. Kern, A. Garcia-Lekue, T. Frederiksen, D. Sanchez-Portal, and A. Arnau, Surveying molecular vibrations during the formation of metal-molecule nanocontacts, Nano Lett. **10**, 657 (2010).

[54] Z. C. Dong, X. L. Zhang, H. Y. Gao, Y. Luo, C. Zhang, L. G. Chen, R. Zhang, X. Tao, Y. Zhang, J. L. Yang, and J. G. Hou, Generation of molecular hot electroluminescence by resonant nanocavity plasmons, Nat. Photonics **4**, 50 (2010).

[55] T.-H. Park and M. Galperin, Self-consistent full counting statistics of inelastic transport, Phys. Rev. B **84**, 205450 (2011).

[56] M. Galperin and A. Nitzan, Raman scattering from biased molecular conduction junctions: The electronic background and its temperature, Phys. Rev. B **84**, 195325 (2011).

[57] Y. Kim, H. Song, F. Strigl, H.-F. Pernau, T. Lee, and E. Scheer, Conductance and Vibrational States of Single-Molecule Junctions Controlled by Mechanical Stretching and Material Variation, Phys. Rev. Lett. **106**, 196804 (2011).

[58] G. Tian, J.-C. Liu, and Y. Luo, Density-Matrix Approach for the Electroluminescence of Molecules in a Scanning Tunneling Microscope, Phys. Rev. Lett. **106**, 177401 (2011).

[59] D. Gelbwaser-Klimovsky, A. Aspuru-Guzik, M. Thoss, and U. Peskin, High-voltage-assisted mechanical stabilization of single-molecule junctions, Nano Lett. **18**, 4727 (2018).

[60] P. Gehring, J. M. Thijssen, and H. S. van der Zant, Single-molecule quantum-transport phenomena in break junctions, Nat. Rev. Phys. **1**, 381 (2019).

[61] X. Bian, Z. Chen, J. K. Sowa, C. Evangeli, B. Limburg, J. L. Swett, J. Baugh, G. A. D. Briggs, H. L. Anderson, J. A. Mol, and J. O. Thomas, Charge-State Dependent Vibrational Relaxation in a Single-Molecule Junction, Phys. Rev. Lett. **129**, 207702 (2022).

[62] M. Imai-Imada, H. Imada, K. Miwa, Y. Tanaka, K. Kimura, I. Zoh, R. B. Jaculbia, H. Yoshino, A. Muranaka, M. Uchiyama, and Y. Kim, Orbital-resolved visualization of single-molecule photocurrent channels, Nature (London) **603**, 829 (2022).

[63] T. L. Cocker, D. Peller, P. Yu, J. Repp, and R. Huber, Tracking the ultrafast motion of a single molecule by femtosecond orbital imaging, Nature (London) **539**, 263 (2016).

[64] P. Salén, M. Basini, S. Bonetti, J. Hebling, M. Krasilnikov, A. Y. Nikitin, G. Shamuilov, Z. Tibai, V. Zhaunerchyk, and V. Goryashko, Matter manipulation with extreme terahertz light: Progress in the enabling THz technology, Phys. Rep. **836-837**, 1 (2019).

[65] M. Müller, N. Martín Sabanés, T. Kampfrath, and M. Wolf, Phase-resolved detection of ultrabroadband THz pulses inside a scanning tunneling microscope junction, ACS Photonics **7**, 2046 (2020).

[66] L. Bi, K. Liang, G. Czap, H. Wang, K. Yang, and S. Li, Recent progress in probing atomic and molecular quantum coherence with scanning tunneling microscopy, Prog. Surf. Sci. **98**, 100696 (2022).

[67] X. Qiu, G. Nazin, and W. Ho, Vibrationally resolved fluorescence excited with submolecular precision, Science **299**, 542 (2003).

[68] L.-L. Nian, T. Wang, and J.-T. Lü, Plasmon squeezing in single-molecule junctions, Nano Lett. **22**, 9418 (2022).

[69] A. Zazunov, D. Feinberg, and T. Martin, Phonon Squeezing in a Superconducting Molecular Transistor, Phys. Rev. Lett. **97**, 196801 (2006).

[70] N. S. Maslova, V. N. Mantsevich, P. I. Arseyev, and I. M. Sokolov, Tunneling current induced squeezing of the single-molecule vibrational mode, Phys. Rev. B **100**, 035307 (2019).

[71] A. I. Lvovsky, Squeezed light, in *Photonics: Scientific Foundations, Technology and Applications*, edited by D. L. Andrews (Wiley, Hoboken, NJ, 2015), Vol. 1, Chap. 5, pp. 121–163.

[72] L.-L. Nian, B. Zheng, and J.-T. Lü, Electrically driven photon statistics engineering in quantum-dot circuit quantum electrodynamics, Phys. Rev. B **107**, L241405 (2023).

[73] W. Vogel and D.-G. Welsch, *Quantum Optics* (Wiley-VCH, Weinheim, 2006), pp. 205–231.

[74] A. Ourjoumtsev, A. Kubanek, M. Koch, C. Sames, P. W. Pinkse, G. Rempe, and K. Murr, Observation of squeezed light from

one atom excited with two photons, Nature (London) **474**, 623 (2011).

[75] M. J. Gullans, Y.-Y. Liu, J. Stehlik, J. R. Petta, and J. M. Taylor, Phonon-Assisted Gain in a Semiconductor Double Quantum Dot Maser, Phys. Rev. Lett. **114**, 196802 (2015).

[76] T. R. Hartke, Y.-Y. Liu, M. J. Gullans, and J. R. Petta, Microwave Detection of Electron-Phonon Interactions in a Cavity-Coupled Double Quantum Dot, Phys. Rev. Lett. **120**, 097701 (2018).

[77] M. J. Gullans, J. M. Taylor, and J. R. Petta, Probing electron-phonon interactions in the charge-photon dynamics of cavity-coupled double quantum dots, Phys. Rev. B **97**, 035305 (2018).

[78] A. Blais, A. L. Grimsmo, S. M. Girvin, and A. Wallraff, Circuit quantum electrodynamics, Rev. Mod. Phys. **93**, 025005 (2021).

[79] F. Herrera and J. Owrutsky, Molecular polaritons for controlling chemistry with quantum optics, J. Chem. Phys. **152**, 100902 (2020).

[80] B. Xiang and W. Xiong, Molecular vibrational polariton: Its dynamics and potentials in novel chemistry and quantum technology, J. Chem. Phys. **155**, 050901 (2021).

[81] F. J. Garcia-Vidal, C. Ciuti, and T. W. Ebbesen, Manipulating matter by strong coupling to vacuum fields, Science **373**, eabd0336 (2021).

[82] T. E. Li, B. Cui, J. E. Subotnik, and A. Nitzan, Molecular polaritonics: Chemical dynamics under strong light–matter coupling, Annu. Rev. Phys. Chem. **73**, 43 (2022).

[83] M. Sánchez-Barquilla, A. I. Fernández-Domínguez, J. Feist, and F. J. García-Vidal, A theoretical perspective on molecular polaritonics, ACS Photonics **9**, 1830 (2022).

[84] K. B. Arnardottir, A. J. Moilanen, A. Strashko, P. Törmä, and J. Keeling, Multimode Organic Polariton Lasing, Phys. Rev. Lett. **125**, 233603 (2020).

[85] J. Tang, J. Zhang, Y. Lv, H. Wang, F. F. Xu, C. Zhang, L. Sun, J. Yao, and Y. S. Zhao, Room temperature exciton–polariton Bose–Einstein condensation in organic single-crystal microribbon cavities, Nat. Commun. **12**, 3265 (2021).

[86] D. M. Coles, N. Somaschi, P. Michetti, C. Clark, P. G. Lagoudakis, P. G. Savvidis, and D. G. Lidzey, Polariton-mediated energy transfer between organic dyes in a strongly coupled optical microcavity, Nat. Mater. **13**, 712 (2014).

[87] K. E. Dorfman and S. Mukamel, Multidimensional photon correlation spectroscopy of cavity polaritons, Proc. Natl. Acad. Sci. USA **115**, 1451 (2018).

[88] Z. Yang, H. H. Bhakta, and W. Xiong, Enabling multiple intercavity polariton coherences by adding quantum confinement to cavity molecular polaritons, Proc. Natl. Acad. Sci. USA **120**, e2206062120 (2023).